Global modeling of high-resolution spectra of the atmospheric gas molecules

V.I. Perevalov,[1] S.A. Tashkun,[1] Vl.G. Tyuterev,[2] and O.M. Lyulin[1]

[1]*Institute of Atmospheric Optics, Siberian Branch of the Russian Academy of Science, Tomsk, Russia*
[2]*Reims University, Reims, France*

Received February 15, 2007

The global calculations of high-resolution molecular spectra using the variational and the effective operator techniques have been analyzed comparatively. The main results on the global modeling of high-resolution spectra of CO_2, N_2O, C_2H_2, H_2O, O_3, and H_2S molecules, obtained at the Laboratory of Theoretical Spectroscopy, IAO SB RAS in collaboration with colleagues from CNRS (France) and NASA (USA) are briefly presented.

Introduction

Numerous applications of high-resolution molecular spectroscopy to atmospheric physics, astrophysics, and various technological investigations require wider spectral ranges, more accurate modeling of high-resolution molecular spectra, and more reliable prediction of such spectra for different isotopic modifications and ambient conditions. In this connection, the interest to the problem of global description of rotational-vibrational molecular spectra in the region from microwave to the visible wavelengths has grown significantly in recent years. The permanently increasing interest to this problem is caused also by the fact that models globally describing spectra in the ground electronic state can be used to obtain new information about high-excited rotational-vibrational states. This capability finds wide range of applications to solving the problems on high-temperature molecular spectra.

Two approaches to the global description of rotational-vibrational molecular spectra are currently being used. The first one is based on the potential energy function, the dipole moment function, and the operator of total kinetic energy of nuclei, as well as on the solution of the Schrödinger equation by variational or other numerical methods. The second approach is based on the method of effective operators using the algebraic technique. The method consists essentially in the construction of the effective Hamiltonian and the corresponding effective dipole moment operator with the aid of the perturbation theory and in the reconstruction of the parameters of these effective operators from experimental spectra. Both of the approaches are being used actively in the Laboratory of Theoretical Spectroscopy at the Institute of Atmospheric Optics SB RAS. This paper presents some results on the global description of high-resolution molecular spectra obtained in our laboratory within the framework of both approaches in collaboration with colleagues from CNRS (France) and NASA (USA).

1. Effective operator approach

We extensively use the effective operator approach in the global description of high-resolution spectra of linear semirigid molecules, such as CO_2, N_2O, and C_2H_2. Within this approach, small unitary transformations $\exp(-iS)$ are used to reduce the initial vibrational-rotational Hamiltonian H_{VR} to the effective Hamiltonian

$$H^{\text{eff}} = \exp(iS) H_{VR} \exp(-iS), \qquad (1)$$

whose matrix in the basis of eigenfunctions of energy operators of harmonic oscillations and a rigid symmetric top is much simpler than the matrix of the initial vibrational-rotational Hamiltonian. Such transformations can be performed, for example, with the aid of the method of contact transformations,[1,2] which is one of the modifications of the degenerate perturbation theory.

In case the normal coordinates are used, matrix elements of the effective Hamiltonian are expressed by simple analytical expressions through parameters and quantum numbers. Usually, researchers try to separate groups of resonantly interacting vibrational states in a molecule and to transform the vibrational-rotational Hamiltonian to the effective Hamiltonian, whose matrix has a block-diagonal form in the basis of vibrational functions of zero approximation. However, in the global description of high-resolution molecular spectra this is not always possible owing to resonance perturbations associated with the

0235-6880/07/05 359-09 $02.00

overlapping polyads, as will be demonstrated below for the N_2O molecule taken as an example.

Calculations become simpler within the effective operator approach due to the possibility of separately diagonalizing every block of the effective Hamiltonian matrix in order to determine eigenvalues and eigenfunctions. Even in the cases, when vibrational states cannot be divided into finite "isolated" groups of resonantly interacting vibrational states, the matrix of the effective Hamiltonian is still simpler than the matrix of the initial vibrational-rotational Hamiltonian.

Calculation of the absorption line intensities can be done within the effective operator approach with the use of the eigenfunctions of the effective Hamiltonian, but it is necessary to use the effective dipole moment operator, which results from the dipole moment operator μ after the same unitary transformations:

$$\mu^{\text{eff}} = \exp(iS)\mu\exp(-iS), \qquad (2)$$

as those used to transform the vibrational-rotational Hamiltonian into the effective Hamiltonian.

In practical applications of this method to modeling high-resolution molecular spectra, most papers omit the transformations associated with the perturbation theory, but, instead, based on the fact that these transformations yield the effective Hamiltonian and the effective dipole moment operator in the form of series in terms of vibrational and rotational operators, write the operator terms of these series based on symmetry requirements. Parameters of these operators are declared empirical parameters and are determined by fitting to experimental values of the transition frequencies (in the case of the effective Hamiltonian) or line intensities (in the case of the effective dipole moment operator).

Recently the algorithms for calculation of high-order-parameters have been realized,[3,4] which allow one to construct *ab initio* effective models from potential functions and dipole moment functions.

1.1. CO_2 molecule

The series of papers[5–21] is devoted to the global modeling of high-resolution spectra of the carbon dioxide molecule and its isotopic modifications. All the papers used the polyad model of the effective Hamiltonian,[5,8,10,22] including contributions up to the sixth order of the perturbation theory. This model takes into account all resonance interactions owing to the following approximate relationships between harmonic frequencies: $\omega_1 \approx 2\omega_2$ and $\omega_3 \approx 3\omega_2$. Parameters of this effective Hamiltonian were determined empirically by the least squares fit from the experimental positions of spectral line centers published in different papers. Each of the isotopic modifications was considered separately. Whenever necessary, the Ritz principle was used for re-calibration of the input experimental transition frequencies with respect to high-accuracy microwave and laser heterodyne data. For all the modifications considered, the modeling accuracy achieved was close to the experimental uncertainty. Table 1 summarizes the model results on the line center positions for various isotopic modifications of the carbon dioxide molecule.

Table 1. Results obtained by modeling positions of the spectral line centers of different isotopic modifications of the CO_2 molecule

Molecule	$^{12}C^{16}O_2$	$^{13}C^{16}O_2$	$^{16}O^{12}C^{18}O$	$^{16}O^{12}C^{17}O$	$^{16}O^{13}C^{18}O$
Number of lines	29000	14650	6600	1800	6411
Number of bands	364	181	72	30	58
RMS deviation, cm^{-1}	0.002	0.002	0.001	0.001	0.002
χ	1.69	2.00	2.15	1.63	1.77
Number of parameters	130	96	73	45	61

Note. RMS deviation is the root-mean-square deviation; χ is the weighted standard deviation.

For modeling the line intensities, we used eigenfunctions of the effective Hamiltonian obtained earlier from the modeling the positions of line centers. Parameters of the effective dipole moment operators were determined from experimental intensities of spectral lines taken from the literature and obtained experimentally by our colleagues.[11,13,14,18–20] We used the serial approach, since line intensities of each series of transitions ΔP, where $P = 2V_1 + V_2 + 3V_3$ is the polyad number, are determined by their own set of the effective dipole moment parameters. Figure 1 shows the isotopic modifications and transition series (spectral ranges), for which the intensities of spectral lines were modeled.

It should be noted that in all cases the obtained sets of effective dipole moment parameters reconstruct experimental intensities accurate to the experimental uncertainty.

The modeling of high-resolution spectra of the carbon dioxide molecule performed has allowed us to compile two versions of the bank of spectral line parameters: CDSD-296 version for atmospheric applications[23] and CDSD-1000 version for high-temperature applications.[24] Both of these versions are available on the web-site of the Institute of Atmospheric Optics and open for free access at http://cdsd.iao.ru (http://cdsd.lpma.jussieu.fr), ftp://ftp.iao.ru/pub/CDSD-296, and ftp://ftp.iao.ru/pub/CDSD-1000.

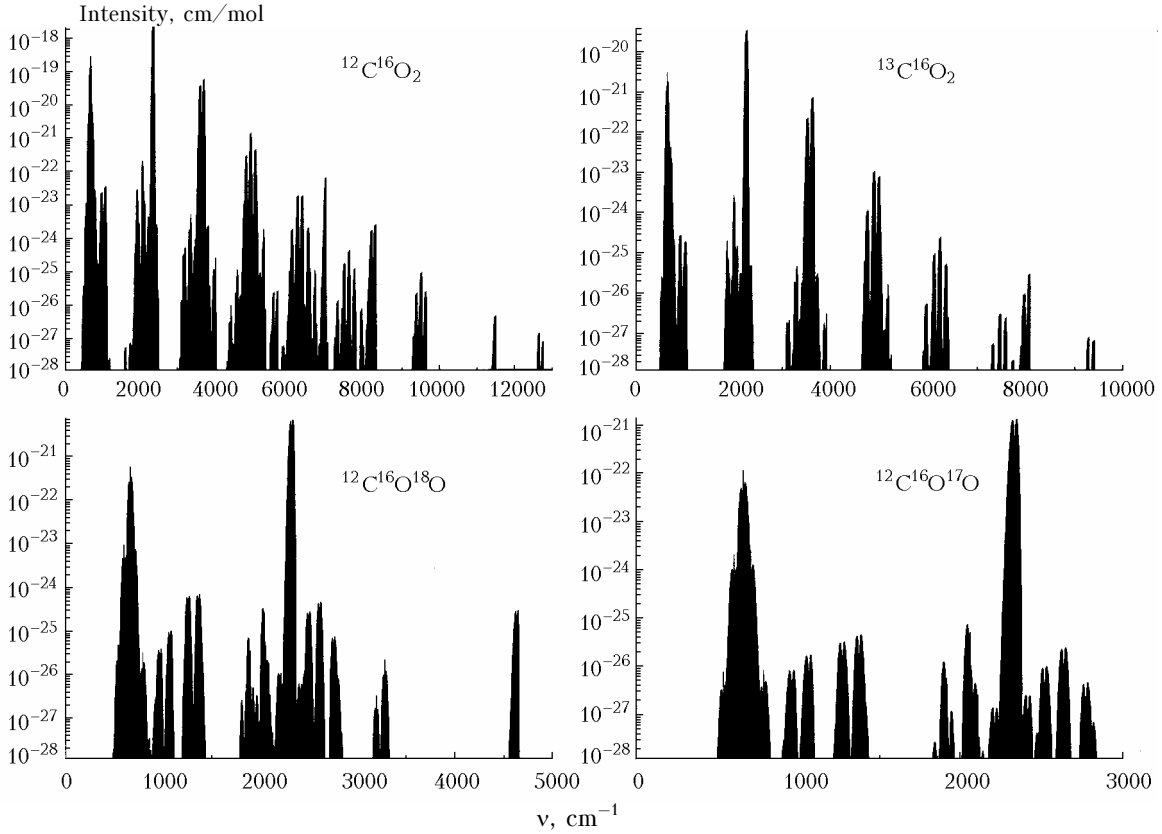

Fig. 1. Spectral regions, in which high-resolution spectra were modeled for isotopic modifications of the carbon dioxide molecule.

1.2. N_2O molecule

At the first stage of the global modeling of high-resolution spectra of the nitrous oxide molecule, the polyad model of the effective Hamiltonian was used.[25] Polyads of vibrational states appear in this molecule due to the following approximate relationship between harmonic frequencies: $\omega_3 \approx 2\omega_1 \approx 4\omega_2$. The polyad model of the effective Hamiltonian explicitly takes into account anharmonic and anharmonic + l-type resonance interactions. The result of modeling the line center positions with the use of this model is presented in Table 2.

Table 2. Model results on the positions of N_2O spectral line centers

Model	Number of parameters	Number of bands	Number of lines	J_{max}	χ	RMS, 10^{-3} cm^{-1}
Polyad	155	250	25000	104	3.16	2.2
Nonpolyad	145	339	28500	104	6.53	12.0

See Notes to Table 1.

The obtained set of parameters of the effective Hamiltonian very well reconstructs positions of the spectral line centers in the most of the bands, but discrepancies between calculated and experimental line centers for some bands lying in the high-frequency spectral region appeared to be very large (up to 1.2 cm^{-1}). Analysis of this situation has shown that the corresponding bands are disturbed by the interpolyad Coriolis and anharmonic resonance interactions.[26–28]

At the second stage, a new nonpolyad model of the effective Hamiltonian was proposed.[29] This model takes into account interpolyad Coriolis and anharmonic resonance interactions. The matrix of this Hamiltonian has no polyad structure, and it should be truncated for diagonalization. To obtain results with the accuracy close to modern experimental data, one has to diagonalize a high dimensionality matrix in the cycle of the inverse problem, which demands a high computer power. Tentative results of modeling the positions of spectral line centers within the framework of the nonpolyad model of the effective Hamiltonian are also presented in Table 2. Both of the models of the effective Hamiltonian were used successfully for analysis of experimental high-resolution spectra of the N_2O molecule.[26–31]

To calculate line intensities for this molecule, eigenfunctions of both models of the effective Hamiltonian were used. Intensities were modeled in a wide spectral region from 20 to 0.98 μm (see Refs. 32–35). The results obtained by modeling are summarized in Table 3, in which the whole spectral region is divided into subregions corresponding to transition series ΔP, where $P = 2V_1 + V_2 + 4V_3$ is the polyad number. For $\Delta P = 1, 3, 5, 6$ only integral band intensities were modeled.[36]

Table 3. Model values of N_2O spectral line intensities

ΔP	Number of parameters	Number of lines	Number of bands	χ	RMS, %
2	11	1136	11	1.3	4.2
4	12	652	10	0.4	
7–9	47	3788	69	1.0	2.9
10	22	4501	26	0.9	12.2
11	2	56	1	1.1	9.5
12	14	832	13	0.6	5.8
13	2	18	1	0.5	11.8
14	8	434	10	0.6	14.5
16	10	568	10	0.6	9.1
18	4	130	3	0.5	9.2

See Notes to Table 1.

1.3. C_2H_2 molecule

The global modeling of high-resolution spectra of the acetylene molecule was performed within the framework of the polyad model of the effective Hamiltonian.[37] The polyad structure of vibrational energy levels in this model is caused by the following approximate relationships between harmonic frequencies:

$$\omega_1 \approx \omega_3 \approx 5\omega_4 \approx 5\omega_5, \quad \omega_2 \approx 3\omega_4 \approx 3\omega_5.$$

The effective Hamiltonian proposed in Ref. 37 was used to fit positions of 9046 lines of 142 bands lying in the region from 50 to 10120 cm^{-1}. As a result, the set of 150 parameters of the effective Hamiltonian has been determined experimentally. These parameters reconstruct the input data with the rms deviation of 0.005 cm^{-1} (see Ref. 38). Figure 2 compares the average (for each band) and rms (for each band as well) deviations of calculated line centers from the experimental values.

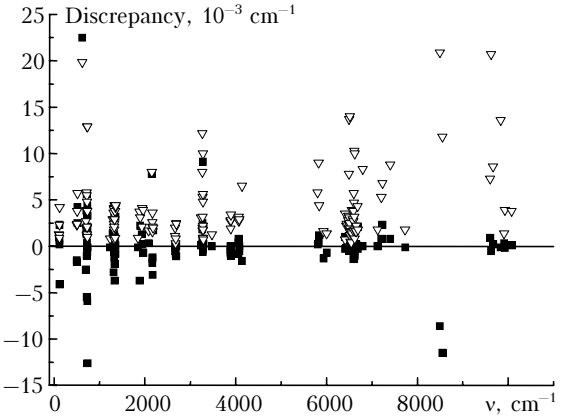

Fig. 2. Comparison of calculated positions of line centers of the C_2H_2 molecule with the experimental values: average (squares) and rms (triangles) deviations for each band included in the fit.

Despite the accuracy of reconstruction of the input experimental data with the aid of the reconstructed set of parameters is rather high, extrapolative and interpolative calculations with this Hamiltonian still yield to analogous calculations for both CO_2 and N_2O molecules in accuracy. The reason is that several important Hamiltonian parameters are absent in our set, because in the literature there is no experimental information needed for their determination. An experiment to fill this gap is planned now.

Line intensities are modeled very well with the aid of eigenfunctions of the effective Hamiltonian obtained. Since acetylene is a tetratomic linear molecule, the equations used to calculate line intensities should be modified significantly as compared to the corresponding equations for thriatomic molecules, as was done in Refs. 39 and 40. Intensities are modeled in a wide spectral range, namely, for transition series $\Delta P = 1$–8 and 10 (see Refs. 40–45). Here the polyad number P is determined through vibrational quantum numbers as follows V_i (i = 1, 2, 3, 4, 5):

$$P = 5V_1 + 3V_2 + 5V_3 + V_4 + V_5.$$

Table 4 presents the results obtained by this modeling.

Table 4. Results on the spectral line intensities of the C_2H_2 molecule obtained by modeling

ΔP series	1	2	3	4	5	6	7	8	10
Region, μm	13.6	7.8	5.0	3.8	3.0	2.5	2.2	1.9	1.5
Number of bands	6	3	15	5	20	9	8	7	4
Number of lines	431	115	535	245	591	665	444	300	269
Number of parameters	4	3	18	8	6	10	11	17	4
RMS, %	3.6	4.4	4.7	1.4	4.2	3.5	3.6	3.5	1.3
χ	0.8	1.0	1.0	0.5	0.6	0.6	0.9	0.5	0.7

See Notes to Table 1.

2. Global calculations of variational type

Rotational-vibrational spectra are usually calculated from the potential energy function and dipole moment functions using the variational approach or other methods close to this approach in formulation of the problem. Most of these methods have a common feature, namely, numerical solution of the quantum-mechanics problem on determination of eigenvalues of the energy operator that depends on $3N - 3$ specially selected vibrational-rotational coordinates. To reduce the size of the matrix of the vibrational-rotational Hamiltonian, various strategies[46–50] are used for its compression and truncation. It should be noted that in the literature the discrete variable representation (DVR) method[51] and the filter diagonalization method, well suited for improving the convergence of eigenvalues of high-excited states,[52] are used quite widely.

In contrast to the algebraic effective operator approach presented in the previous sections, the variational and related approaches employ the integro-differential technique for calculation of matrix elements. These two theoretical approaches use, as a rule, significantly different coordinates and molecule-fixed axes and have different extrapolation capabilities. The detailed comparison of these approaches can be found in the review presented in Ref. 53.

One of the advantages of the variational approach is the conceptual simplicity in prediction of spectra of isotopic modifications of a molecule. Within the framework of the Born–Oppenheimer approximation, the potential energy surface and the dipole moment surface are isotopically invariant, and the operator of kinetic energy for triatomic molecules is exactly determined.[46,47,50] These statements remain valid even in the case of relativistic corrections are to be taken into account.[54,62]

Thus, within the framework of the Born–Oppenheimer approximation, to calculate spectra of an isotopic modification of a molecule, by use of the variational approach it is sufficient only to change masses in the kinetic energy operator, keeping the procedure of the following calculations nearly unchanged. At the same time, within the framework of the effective operator approach, which uses the mass-dependent normal coordinates, it is necessary to re-determine parameters of both the effective Hamiltonian and the effective dipole moment operator, and in some cases (most often, if the molecular symmetry reduces) it is also necessary to change the scheme and nature of the perturbations.

It should be noted that to apply variational calculations to solution problems in high-resolution spectroscopy, both the potential energy surface and the dipole moment surface should be set very accurately. Such surfaces have been determined recently through *ab initio* calculations and empirical optimization for several triatomic molecules, such as water vapor molecule,[54–57] ozone,[58–61] hydrogen sulfide,[62–66] and some other molecules. If higher approximations are taken into account, the separation of electronic states leads to mass-dependent corrections to the potential energy surface, the main of which are the so-called diagonal Born–Oppenheimer corrections,[54,62] as well as to nonadiabatic corrections to the kinetic energy operator of a molecule.[67,68]

In recent years, the global variational, DVR, and related calculations have achieved such a high accuracy that they have became really useful for analysis of high-resolution molecular spectra and prediction of high-excited states. Nevertheless, for low and medium values of quantum numbers they significantly yield to the effective operator calculations in accuracy. The effective operator approach still remains the main supplier of data for banks of spectroscopic information. However, the variational approach has undoubted advantages in the cases that perturbation series are poorly convergent, for example, for nonrigid molecules, for which the effective operator approach requires significant modifications associated with the summation of series and nonpolynomial representations.[4] Thus, the effective operator approach and the variational approach should be considered as complementary.

2.1. H_2O molecule

Partridge and Schwenke are authors of the first impressive breakthrough in the global calculation of high-resolution molecular spectra.[54,56] Their calculations for water vapor molecule were based on the *ab initio* potential energy and dipole moment surfaces. The potential energy surface was then optimized with the use of experimental values of the line center positions for $J \le 5$, and it included mass-dependent corrections for isotopic modifications with the hydrogen atom substituted with the deuterium atom. The data bank compiled by use of these calculations[54,56] and including about $3 \cdot 10^8$ spectral lines is widely used for assignment of spectra recorded in chambers with a long optical path,[69–71] for interpretation of high-temperature spectra obtained under laboratory conditions and from sunspots,[72] and spectra of isotopic modifications.[73–75] Recently the team of the Institute of Applied Physics RAS (Nizhnii Novgorod, Russia) and the Tennyson's group[55,57,76] have succeeded in refinement of the *ab initio* potential energy surface of water vapor molecule in the region of high energies by use of an extended electron basis and taking into consideration the relativistic and radiation corrections, as well as adiabatic and nonadiabatic corrections calculated by Schwenke.[68] The review of these investigations can be found elsewhere.[76]

The variational calculation of intensities from the *ab initio* dipole moment surface[54,56] yields the globally acceptable agreement with the experiment, but the discrepancy ~20% for some strong bands (in particular, ν_1) makes the accuracy of this calculation insufficient for atmospheric and meteorological applications in some frequency ranges. Recently[77] an attempt to optimize the dipole moment function has been undertaken by using simultaneously *ab initio* calculations and the vast array of experimental data on the line strengths. This has allowed one to improve description of line intensities of fundamental and some other bands in the low- and mid-frequency ranges. Figure 3 exemplifies these results with the $3\nu_2$ band of the main isotopic modification. In Fig. 3, one can compare experimental intensities obtained in the more recent paper by Jenouvrier et al.[78] with the values calculated using the Partridge–Schwenke *ab initio* dipole moment function[56] and new optimized dipole moment function.[77]

The problem of empirical optimization of the dipole moment surface for modeling the intensities in the high-frequency spectral region still remains open owing to the lack of experimental information and

contradictory data of different authors. To achieve progress in this field, more comprehensive accurate measurements on long optical paths are needed.

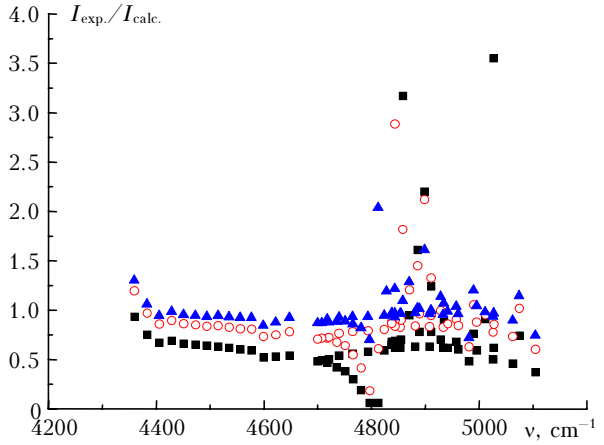

Fig. 3. Comparison of experimental and calculated intensities of lines of the $3\nu_2$ band ($K_a'' = 0$ series) of the main isotopic modification of water vapor molecule $H_2{}^{16}O$. Experiment by Jenouvrier et al.[78]; calculations: (closed squares) Ref. 54; (circles) Ref. 56; (triangles) Ref. 77.

2.2. O_3 molecule

The development of programs realizing the variational approach has allowed the rather good convergence of energies and wave functions in the vibrational-rotational basis to be achieved. In the best cases, convergence errors for positions of the spectral line centers are ~0.01–0.001 cm^{-1}. However, typically the *ab initio* potential energy surface give a much larger error in calculated of positions of the spectral line centers. To improve the accuracy of calculations, parameters of the potential energy and the dipole moment surfaces are optimized taking into account experimental line positions and intensities. This formulation of the inverse problem appears to be more complicated as compared to the empirical determination of parameters of the effective Hamiltonians and the effective dipole moment operators. These surfaces should also provide for correct physical properties of molecules, manifesting themselves in experiments of various types, for example, in chemistry and kinetics (dissociation threshold, asymptotics, potential barriers, etc.).

The improvement achieved in the global modeling of high-resolution spectra of the ozone molecule[58–61] is connected with the use of the specific method of empirical optimization of the potential energy surface. Namely, the least-squares method with flexible additional conditions was used. These additional conditions play the role of penalty functions at a nonphysical behavior of the potential energy surface during the optimization. Use of these conditions enables one to intercept the gradients in the space of parameters, that would lead to nonphysical behavior of the potential energy surface. That is, using these conditions, it is possible to avoid false minima and nonrealistic asymptotics, as well as to overcome the slipping of the least-squares procedure to unacceptable local minima of the weighted standard deviation. The combination of different strategies in selection of the penalty functions has allowed the optimization to be performed with the observance of physically justified conditions.[59]

Predicted energies of high-excited states obtained with the empirically reconstructed potential energy surface of the ozone molecule[58–60] turned out to be very useful for interpretation of the absorption bands in the case of the main isotopic modification, as well as for assignment of the spectrum of ozone enriched with the ^{18}O oxygen isotope (see Ref. 79). In this case, the spectrum consists of overlapping bands of six isotopic modifications and the density of lines in this spectrum is from 200 to 300 lines per 1 cm^{-1}. Global calculations favor identification and localization of resonance perturbations by "dark" (not observed experimentally) states. Ultimately, this allowed the analysis and modeling (with experimental accuracy) of about 35 new bands in ozone spectra.[79,80] For a comparison, Table 5 presents experimental and calculated values of the band centers for the asymmetric $^{16}O^{16}O^{18}O$ isotopic modification of the ozone molecule.

Line positions of the ozone molecule predicted with the aid of variational calculations using the potential energy surface from Refs. 58 and 59 turned out to be very useful for assignment and analysis of the spectrum of this molecule near 1.5 μm recorded with the cavity ring down spectroscopy (CRDS) (see Ref. 80). The very sensitive CRDS method makes it possible to observe the bands formed by transitions between high-excited vibration-rotation states, whose energies for the ozone molecule are only 20% lower than the dissociation threshold. These measurements have confirmed a good agreement between the calculated and experimental line positions.

Table 5. Experimental[79] and calculated[60] values of band centers for the asymmetric isotopic modification $^{16}O^{16}O^{18}O$ of the ozone molecule

Band	Exp., cm^{-1}	Exp. – Calc., cm^{-1}	Band	Exp., cm^{-1}	Exp.– Calc., cm^{-1}
ν_2	684.6134	0.00	$3\nu_3$	2998.8751	0.04
ν_3	1028.1118	0.00	$\nu_1 + 2\nu_3$	3060.5647	0.12
ν_1	1090.3538	0.00	$2\nu_1 + \nu_3$	3148.1456	0.09
$2\nu_2$	1366.7375	0.00	$\nu_1+2\nu_2+\nu_3$	3403.6700	0.05
$\nu_2 + \nu_3$	1696.8848	0.00	$\nu_2 + 3\nu_3$	3636.9341	0.02
$\nu_1 + \nu_2$	1767.2256	0.00	$4\nu_3$	3932.992	–0.10
$2\nu_3$	2028.7169	0.01	$\nu_1 + 3\nu_3$	4002.4123	0.42
$\nu_1 + \nu_3$	2090.3394	0.00	$2\nu_1 + 2\nu_3$	4092.4675	–0.06
$2\nu_1$	2172.5182	–0.21	$5\nu_3$	4824.3836	0.14

2.3. H_2S molecule

The most accurate potential energy surface for the H_2S molecule[63] was obtained within the framework of the same approach as for the O_3 molecule. The fitting involved 4175 rotational-vibrational energy levels with $J_{max} = 15$ and $K_{a\,max} = 15$ for seven isotopic modifications ($H_2{}^{32}S$, $H_2{}^{33}S$, $H_2{}^{34}S$, $D_2{}^{32}S$, $D_2{}^{34}S$, $HD^{32}S$, and $HD^{34}S$). As a result, the rms deviation of calculated line positions from the experimental ones of 0.05 cm^{-1} was achieved for all 73 bands of the isotopic modifications considered, the rms deviation for line positions was 0.03 cm^{-1}.

The hydrogen sulfide molecule is known for the anomalous behavior of line intensities upon the transition from fundamental bands to the overtone and combination ones (see Refs. 81, 64 and references therein). Until recently, all attempts to explain these anomalies based on calculations that do not use empirical data failed. The earlier *ab initio* calculations yielded the intensity of the ν_3 band that appeared to be an order of magnitude higher than its experimental value. Moreover, the intensity distribution over rotational-vibrational lines differed considerably from the observed one. In particular, the calculation gave an incorrect shape of the *Q*-branch. The first derivatives of the dipole moment with respect to the normal coordinates determined from the *ab initio* calculations differed significantly from the experimental values. The new *ab initio* investigations[64,65] have shown that to describe the anomalous behavior of line intensities of the H_2S molecule, very accurate dipole moment surface is necessary, because it is close to plane near the equilibrium configuration, and therefore the calculated line intensities of the fundamental ν_3 and ν_1 absorption bands are very sensitive to the accuracy of determination and to the shape of this surface.

Recent variational calculations[66] with the use of the improved dipole moment surface for the hydrogen sulfide molecule have allowed the anomalies in the behavior of line intensities to be explained not only for the most abundant isotopic modifications, but also for the deuterated isotopic modifications HDS and D_2S. To test the quality of isotopic extrapolation of both the potential energy surface[63] and the dipole moment surface[66] of the hydrogen sulfide molecule, the group at Reims University (Reims, France) has initiated the experimental project.[82] The experimental results obtained within this project turned out to be in a good agreement with the predictions, which favored the understanding of the cause of the intensity anomaly.

As an example, Figure 4 compares a fragment of the global predictions of the spectrum[66] (Fig. 4*a*) with the more recent experimental spectrum (Fig. 4*b*). To draw the predicted spectrum (Fig. 4*a*), corrections to line positions (Fig. 4*c*) were used.

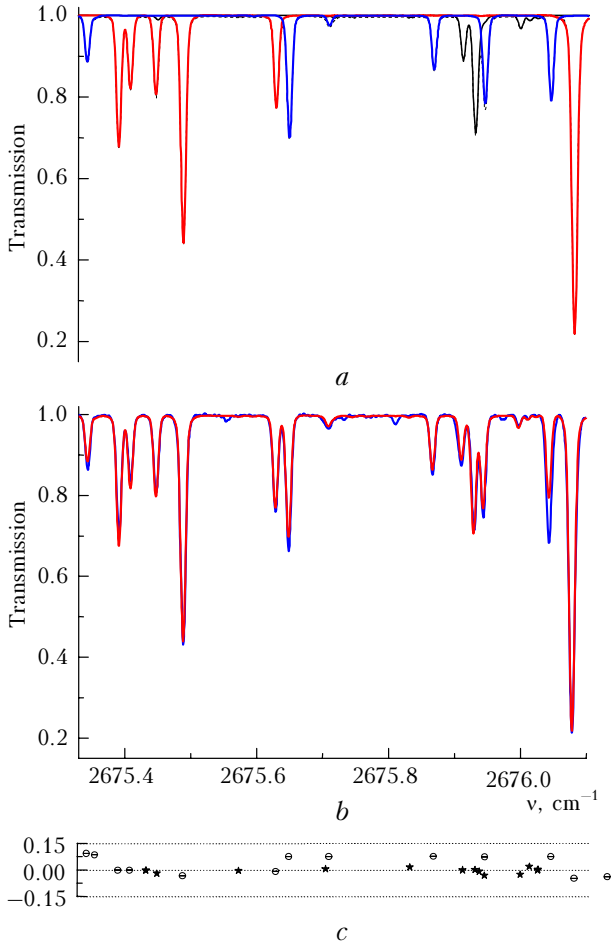

Fig. 4. Comparison of the predicted spectrum (*a*) of a mixture of H_2S, HDS и D_2S (*a*) with the experimental one[82] (*b*); *a*: (black curve) H_2S, (red curve) D_2S, (blue curve) HDS; *b*: (red curve) calculation, (blue curve) experiment; *c*: corrections to line positions in cm^{-1} are plotted on the vertical scale.

Conclusions

This review presents a brief comparative analysis of the variational approach and the effective operator approach used at the Laboratory of Theoretical Spectroscopy, IAO SB RAS (Russia) in collaboration with colleagues from CNRS (France) and NASA (USA) in global modeling of high-resolution molecular spectra. The paper presents also the main results on the global modeling of high-resolution spectra of the CO_2, N_2O, C_2H_2, H_2O, O_3, and H_2S molecules obtained by during the past decade. One of the practical goals of this study is the compilation of banks of spectral line parameters with an accuracy of 1 to 10% for line intensities and 0.01–0.001 cm^{-1} (with the use of effective models) and 0.1–0.01 cm^{-1} (with the use of potential functions) for positions of the line centers. To date the global modeling has been already used for development of two versions of the data bank of spectral line parameters for the carbon dioxide molecule: CDSD-296 version for atmospheric applications[23] and CDSD-1000 version

for high-temperature applications.[24] As follows from the paper, our investigations are close to the compilation of data banks of spectral line parameters with the above accuracy characteristics for the N_2O and C_2H_2 molecules.

From the viewpoint of basic investigations, global calculations favor the understanding of the structure of high-excited states, the study of their qualitative variations, and dynamic processes associated with the intramolecular energy transfer and dissociation.

Acknowledgements

The authors are grateful to J.-L. Teffo for cooperation in modeling of high-resolution spectra of linear molecules and to D.W. Schwenke and M. Ray for cooperation in global variational calculations. The authors are also grateful to A. Barbe, A. Campargue, S. Mikhailenko, M.-R. De Backer-Barilly, J. Vander Auwera, L. Régalia-Jarlot, L. Daumont, D. Bailly, A. Jenouvrier, J.-Y. Mandin, V. Dana, D. Jacquemart, C. Claveau, A. Valentin, S.-M. Hu, Y. Ding, L. Wang, A.W. Liu, and Yu. Borkov, co-authors of the most of the results presented in this paper.

References

1. M.R. Aliev and J.K.G. Watson, Mol. Spectrosc.: Modern Res. **3**, 1–67 (Academic Press, Orlando, 1985).
2. Vl.G. Tyuterev and V.I. Perevalov, Chem. Phys. Lett. **74**, No. 3, 494–502 (1980).
3. Vl.G. Tyuterev, S.A. Tashkun, and H. Seghir, Proc. SPIE **5311**, 164–175 (2004).
4. V.I. Starikov and Vl.G. Tyuterev, *Intramolecular Interactions and Theoretical Methods in Spectroscopy of Nonrigid Molecules* (SB RAS Publishing House, Tomsk, 1997), 232 pp.
5. J.-L. Teffo, O.N. Sulakshina, and V.I. Perevalov, J. Mol. Spectrosc. **156**, No. 1, 48–64 (1992).
6. V.I. Perevalov, E.I. Lobodenko, O.M. Lyulin, and J.-L. Teffo, J. Mol. Spectrosc. **171**, No. 2, 435–452 (1995).
7. J.-L. Teffo, O.M. Lyulin, V.I. Perevalov, and E.I. Lobodenko, J. Mol. Spectrosc. **187**, No. 1, 28–41 (1998).
8. S.A. Tashkun, V.I. Perevalov, J.-L. Teffo, L.S. Rothman, and Vl.G. Tyuterev, J. Quant. Spectrosc. and Radiat. Transfer **60**, No. 5, 785–801 (1998).
9. S.A. Tashkun, V.I. Perevalov, J.-L. Teffo, and Vl.G. Tyuterev, J. Quant. Spectrosc. and Radiat. Transfer **62**, No. 5, 571–598 (1999).
10. S.A. Tashkun, V.I. Perevalov, J.-L. Teffo, M. Lecoutre, T.R. Huet, A. Campargue, D. Bailly, and M.P. Esplin, J. Mol. Spectrosc. **200**, No. 2, 162–176 (2000).
11. J.-L. Teffo, C. Claveau, Q. Kou, G. Guelachvili, A. Ubelmann, V.I. Perevalov, and S. Tashkun, J. Mol. Spectrosc. **201**, No. 2, 249–255 (2000).
12. S.A. Tashkun, V.I. Perevalov, and J.-L. Teffo, J. Mol. Spectrosc. **210**, No. 1, 137–145 (2001).
13. J.-L. Teffo, L. Daumont, C. Claveau, A. Valentin, S.A. Tashkun, and V.I. Perevalov, J. Mol. Spectrosc. **213**, No. 1, 145–152 (2002).
14. J.-L. Teffo, L. Daumont, C. Claveau, A. Valentin, S.A. Tashkun, and V.I. Perevalov, J. Mol. Spectrosc. **219**, No. 2, 271–281 (2003).
15. Y. Ding, V.I. Perevalov, S.A. Tashkun, J.-L. Teffo, A.-W. Liu, and S.-M. Hu, J. Mol. Spectrosc. **222**, No. 2, 276–283 (2003).
16. Y. Ding, P. Macko, D. Romanini, V.I. Perevalov, S.A. Tashkun, J.-L. Teffo, S.-M. Hu, and A. Campargue, J. Mol. Spectrosc. **226**, No. 2, 146–160 (2004).
17. Z. Majcherova, P. Macko, D. Romanini, V.I. Perevalov, S.A. Tashkun, J.-L. Teffo, and A. Campargue, J. Mol. Spectrosc. **230**, No. 1, 1–21 (2005).
18. L. Wang, V.I. Perevalov, S.A. Tashkun, A.-W. Liu, and S.-M. Hu , J. Mol. Spectrosc**. 233**, No. 2, 297–300 (2005).
19. L. Wang, V.I. Perevalov, S.A. Tashkun, Y. Ding, and S.-M. Hu, J. Mol. Spectrosc. **234**, No. 1, 84–92 (2005).
20. J. Vander Auwera, C. Claveau, J.-L. Teffo, S.A. Tashkun, and V.I. Perevalov, J. Mol. Spectrosc. **235**, No. 1, 77–83 (2006).
21. B.V. Perevalov, S. Kassi, D. Romanini, V.I. Perevalov, S.A. Tashkun, and A. Campargue, J. Mol. Spectrosc. **241**, No. 1, 90–100 (2007).
22. A. Chedin, J. Mol. Spectrosc. **76**, Nos. 1–3, 430–491 (1979).
23. S.A. Tashkun, V.I. Perevalov, and J.-L. Teffo, in: *Proc. the NATO Advanced Research Workshop on Remote Sensing of the Atmosphere for Environmental Security, Rabat, Morocco, 2005*, ed. by A. Perrin, N. BenSari-Zizi, and J. Demaison (Springer–Verlag, 2006), pp. 161–170.
24. S.A. Tashkun, V.I. Perevalov, J.-L. Teffo, A.D. Bykov, and N.N. Lavrentieva, J. Quant. Spectrosc. and Radiat. Transfer **82**, Nos. 1–4, 165–196 (2003).
25. J.-L. Teffo, V.I. Perevalov, and O.M. Lyulin, J. Mol. Spectrosc. **168**, No. 2, 390–403 (1994).
26. A. Campargue, G. Weirauch, S.A. Tashkun, V.I. Perevalov, and J.-L. Teffo, J. Mol. Spectrosc. **209**, No. 2, 198–206 (2001).
27. Y. Ding, V.I. Perevalov, S.A. Tashkun, J.-L. Teffo, S. Hu, E. Bertseva, and A. Campargue, J. Mol. Spectrosc. **220**, No. 1, 80–86 (2003).
28. E. Bertseva, A. Campargue, V.I. Perevalov, and S.A. Tashkun, J. Mol. Spectrosc. **226**, No. 2, 196–200 (2004).
29. S.A. Tashkun, V.I. Perevalov, and J.-L. Teffo, in: *Abstracts of Int. Workshop on Atmospheric Spectroscopy Application, Moscow, August, 2002* (Institute of Atmospheric Optics, Tomsk, 2002), pp. 41.
30. L. Wang, V.I. Perevalov, S.A. Tashkun, B. Gao, L.-Y. Hao, and S.-M. Hu, J. Mol. Spectrosc. **237,** No. 2, 129–136 (2006).
31. A.W. Liu, S. Kassi, P. Malara, D. Romanini, V.I. Perevalov, S.A. Tashkun, S.-M. Hu, and A. Campargue, J. Mol. Spectrosc. (in press).
32. O.M. Lyulin, V.I. Perevalov, and J.-L. Teffo, J. Mol. Spectrosc. **180**, No. 1, 72–74 (1996).
33. L. Daumont, J. Vander Auwera, J.-L. Teffo, V.I. Perevalov, and S.A. Tashkun, J. Mol. Spectrosc. **208**, No. 2, 281–291 (2001).
34. L. Daumont, C. Claveau, M.-R. De Backer-Barilly, A. Hamdouni, L. Regalia-Jarlot, J.-L. Teffo, S.A. Tashkun, and V.I. Perevalov, J. Quant. Spectrosc. and Radiat. Transfer **72**, No. 1, 37–55 (2002).
35. L. Daumont, J. Vander Auwera, J.-L. Teffo, V.I. Perevalov, and S.A. Tashkun, J. Quant. Spectrosc. and Radiat. Transfer **104**, No. 3, 342–356 (2007).
36. O.M. Lyulin, V.I. Perevalov, and J.-L. Teffo, J. Mol. Spectrosc. **174**, No. 2, 566–580 (1995).
37. V.I. Perevalov, E.I. Lobodenko, and J.-L. Teffo, Proc. SPIE **3090**, 143–149 (1997).
38. O.M. Lyulin, V.I. Perevalov, and J.-L. Teffo, Proc. SPIE **5311**, 134–143 (2004).

39. V.I. Perevalov, O.M. Lyulin, and J.-L. Teffo, Atmos. Oceanic Opt. **14**, No. 9, 730–738 (2001).
40. V.I. Perevalov, O.M. Lyulin, D. Jacquemart, C. Claveau, J.-L. Teffo, V. Dana, J.-Y. Mandin, and A. Valentin, J. Mol. Spectrosc. **218**, No. 2, 180–189 (2003).
41. O.M. Lyulin and V.I. Perevalov, Atmos. Oceanic Opt. **17**, No. 7, 485–488 (2004).
42. O.M. Lyulin, V.I. Perevalov, J.-Y. Mandin, V. Dana, D. Jacquemart, L. Régalia-Jarlot, and A. Barbe, J. Quant. Spectrosc. and Radiat. Transfer **97**, No. 1, 81–98 (2006).
43. D. Jacquemart, N. Lacome, J.-Y. Mandin, V. Dana, O.M. Lyulin, and V.I. Perevalov, J. Quant. Spectrosc. and Radiat. Transfer **103**, No. 3, 478–495 (2007).
44. O.M. Lyulin, V.I. Perevalov, J.-Y. Mandin, V. Dana, F. Gueye, X. Thomas, P. Von der Heyden, D. Décatoire, L. Régalia-Jarlot, D. Jacquemart, and N. Lacome, J. Quant. Spectrosc. and Radiat. Transfer **103**, No. 3, 496–523 (2007).
45. O.M. Lyulin, V.I. Perevalov, F. Gueye, J.-Y. Mandin, V. Dana, X. Thomas, P. Von der Heyden, L. Régalia-Jarlot, and A. Barbe, J. Quant. Spectrosc. and Radiat. Transfer **104**, No. 1, 133–154 (2007).
46. S. Carter and N.C. Handy, J. Chem. Phys. **87**, No. 7, 4294–4301 (1987).
47. J. Tennyson, S. Miller, and J.R. Henderson, *Methods in Computational Chemistry* (Plenum, New York, 1992), Vol. 4.
48. P. Jensen, J. Mol. Spectrosc. **128**, No. 2, 478–501 (1988).
49. D.W. Schwenke, J. Phys. Chem. **100**, No. 8, 2867–2884 (1996).
50. P. Jensen and P.R. Bunker, eds., *Computational Molecular Spectroscopy* (Wiley & Sons, Chichester, 2000), 670 pp.
51. S.E. Choi and J.C. Light, J. Chem. Phys. **97**, No 10, 7031–7054 (1992).
52. V.A. Mandelstam and H.S. Taylor, J. Chem. Phys. **106**, No. 12, 5085–5090 (1997).
53. Vl.G. Tyuterev, Atmos. Oceanic Opt. **16**, No. 3, 220–231 (2003).
54. H. Partridge and D.W. Schwenke, J. Chem. Phys. **106**, No. 11, 4618–4639 (1997).
55. O.L. Polyansky, O.L. Csaszar, S.V. Shirin, N.F. Zobov, P. Barletta, J. Tennyson, D.W. Schwenke, and P.J. Knowles, Science **299**, 539–542 (2003).
56. D.W. Schwenke and H. Partridge, J. Chem. Phys. **113**, No. 16, 6592–6597 (2000).
57. S.V. Shirin, O.L. Polyansky, N.F. Zobov, P. Barletta, and J. Tennison, J. Chem. Phys. **118**, No. 5, 2124–2129 (2003).
58. Vl.G. Tyuterev, S.A. Tashkun, P. Jensen, A. Barbe, and T. Cours, J. Mol. Spectrosc. **198**, No. 1, 57–76 (1999).
59. Vl.G. Tyuterev, S.A. Tashkun, D.W. Schwenke, P. Jensen, T. Cours, A. Barbe, and M. Jacon, Chem. Phys. Lett. **316**, Nos. 3–4, 271–279 (2000).
60. Vl.G. Tyuterev, S.A. Tashkun, D.W. Schwenke, and A. Barbe, Proc. SPIE **5311**, 176–184 (2004).
61. R. Siebert, P. Fleurat-Lessard, R. Schinke, M. Bittererova, and S.C. Farantos, J. Chem. Phys. **116**, No. 22, 9749–9776 (2002).
62. G. Tarczay, A.G. Csaszar, O.L. Polyanskii, and J. Tennyson, J. Chem. Phys. **115**, No. 11, 1229–1242 (2001).
63. Vl.G. Tyuterev, S.A. Tashkun, and D.W. Schwenke, Chem. Phys. Lett. **348**, Nos. 3–4, 223–234 (2001).
64. T. Cours, P. Rosmus, and Vl.G. Tyuterev, Chem. Phys. Lett. **331**, Nos. 2–4, 317–322 (2000).
65. T. Cours, P. Rosmus, and Vl.G. Tyuterev, J. Chem. Phys. **117**, No. 11, 5192–5208 (2002).
66. Vl.G. Tyuterev, L. Regalia-Jarlot, D.W. Schwenke, S.A. Tashkun, and Yu.G. Borkov, Comptes Rendus. Phys. **5**, 189–199 (2004).
67. P.R. Bunker and R.E. Moss, J. Mol. Spectrosc. **80**, No. 1, 217–228 (1980).
68. D.W. Schwenke, J. Phys. Chem. A **105**, No. 11, 2352–2360 (2001).
69. L.P. Giver, C. Chackerian, Jr., and P. Varanasi, J. Quant. Spectrosc. and Radiat. Transfer **66**, No. 1, 101–105 (2000).
70. D.W. Schwenke, J. Mol. Spectrosc. **190**, No. 2, 397–402 (1998).
71. M. Carleer, M. Jenouvrier, A.C. Vandaele, P. Bernath, M.-F. Mérienne, R. Colin, N.F. Zobov, O.L. Polyansky, J. Tennyson, and V.A. Savin, J. Chem. Phys. **111**, No. 6, 2444–2450 (1999).
72. N.F. Zobov, O.L. Polyansky, J. Tennyson, S.V. Shirin, R. Nassar, T. Hirao, P.F. Bernath, and L. Wallace, Astrophys. J. **530**, No. 2, 994–998 (2000).
73. O. Naumenko, A. Campargue, E. Bertseva, and D. Schwenke, J. Mol. Spectrosc. **201**, No. 2, 297–309 (2000).
74. S.N. Mikhailenko, Vl.G. Tyuterev, and G. Mellau, J. Mol. Spectrosc. **217**, No. 2, 195–211 (2003).
75. G. Mellau, S.N. Mikhailenko, E.N. Starikova, S.A. Tashkun, H. Over, and Vl.G. Tyuterev, J. Mol. Spectrosc. **224**, No. 1, 32–60 (2004).
76. J. Tennyson, Phys. Scr. **73**, No. 1, C53–C56 (2006).
77. S.A. Tashkun, D.W. Schwenke, and Vl.G. Tyuterev, in: *Abstracts of the Nineteenth Colloquium on High Resolution Molecular Spectroscopy*, Universidad de Salamanca, Salamanca (2005), p. 412.
78. A. Jenouvrier, L. Daumont, L. Regalia-Jarlot, V.G. Tyuterev, M. Carleer, A.C. Vandaele, S. Mikhailenko, and S. Fally, J. Quant. Spectrosc. and Radiat. Transfer (in press).
79. Barbe, M.R. De Backer-Barilly, Vl.G. Tyuterev, and S.A. Tashkun, Appl. Opt. **42**, No. 25, 5136–5139 (2003).
80. Campargue, S. Kassi, D. Romanini, A. Barbe, M.R. De Backer-Barilly, and Vl.G. Tyuterev, J. Mol. Spectrosc. **240**, No. 1, 1–13 (2006).
81. L.R. Brown, J.A. Crisp, D. Crisp, O.V. Naumenko, M.A. Smirnov, L.N. Sinitsa, and A. Perrin, J. Mol. Spectrosc. **188**, No. 2, 148–162 (1998).
82. L. Régalia-Jarlot, Vl.G. Tyuterev, Yu. Borkov, J. Malicet, X. Thomas, and P. Von der Heyden, in: *Abstracts of the Eighteenth Colloquium on High Resolution Molecular Spectroscopy,* Université de Bourgogne, Dijon (2003), p. 133.